Theory of the Turbulent Drift Friction Layer of the Ocean

V. A. SUKHORUKOV AND N. V. DMITRIEV

Computing Center, Siberian Division of the USSR, Academy of Sciences, Novosibirsk, USSR

(Manuscript received 6 February 1989, in final form 27 December 1989)

ABSTRACT

The paper proposes a theory of the stationary turbulent drift friction layer that, under the conditions of stable stratification, can appear as the upper mixed layer (UML) of the ocean or as one mixed to the bottom in shallow water. An analytical solution of the drift current equations is obtained as an infinite power series valid for the vertical turbulence exchange coefficient of arbitrary form. General properties of the solution are derived in the form of asymptotic theorems. These state that two types of dynamic processes can form, depending on the free-slip or no-slip conditions at the lower boundary of the drift friction layer at small dimensionless depth. With the free-slip condition, the currents are transverse to the wind direction and the stress distribution is linear in the whole layer. With the no-slip condition, the currents are along the wind direction and the stress distribution is constant in the whole layer as well. Based on this model of vertical turbulent exchange, including equations of turbulent kinetic energy and dissipation of turbulent kinetic energy, the first type is shown to be inherent in the UML when a dimensionless stratification parameter increases, while the second type applies to shallow water where drift currents penetrate to the bottom. The possible formation of a layer with a linear velocity profile and constant turbulence values in the second type is discussed. Analytical models describing both types of these processes are suggested.

1. Introduction

The theory of stationary drift currents began with the work of Ekman (1905). It is concerned with analytical solutions of drift current equations (DCE) with a constant coefficient of vertical turbulent exchange (VTE) and a variable coefficient that preceded Prandtl's formula. Ekman examined the problem with a no-slip condition at the lower boundary and showed that the velocity vector tends to turn towards the wind direction in the whole layer as depth decreases. Nomitsu (1933) studied the same problem with the free-slip condition and showed that the velocity vector of drift currents tends to turn transverse to the wind direction in the whole layer as depth decreases while, when deepening, the solution approaches the Ekman solution (1905) for an infinitely deep ocean. When the ratio between the layer depth, H, and the depth of the Ekman friction layer, D ($D = \pi\sqrt{2K_0/f}$), is small, $H/D < 1$, there are two types of solutions depending on the lower boundary condition. When the ratio H/D is large, the solution is independent of the boundary condition.

Later, analytical solutions of DCE with variable VTE coefficient were studied; they are reviewed by Brown (1978). Among them, singular problems were investigated where the VTE coefficient is zero at the lower boundary of the area. In a singular problem, the boundary condition need not be given at the degeneration point and as a solution a restricted branch is selected. The solutions of singular problems may have no physical applications. Dotsenko (1971) showed by analytical methods that the direction and amplitude of drift velocity are monotonic functions of depth for a VTE coefficient of arbitrary form.

In the paper by Sukhorukov and Dmitriev (1983) DCE is solved analytically with the VTE coefficient represented as an infinite power series (one analytical function). It is well known that any continuous function can be uniquely approximated by a power series to any preassigned accuracy. Hence, the solutions obtained are valid for the coefficient eddy viscosity of arbitrary form. General properties of the solution are formulated as three asymptotic theorems stating that when the ratio H/D is small the drift velocity vector tends to turn towards and transverse to the wind direction and the friction stress approaches constant or linear distribution throughout the layer depending on the lower boundary no-slip or free-slip condition satisfied, respectively (Sukhorukov and Dmitriev 1984, 1986).

Observations in the ocean give evidence for the free-slip condition at the lower boundary of the surface mixed layer (Nikiforov 1961; Lacomb et al. 1972). Data taken from a laboratory buoy in summer in the Mediterranean Sea showed the drift velocity vector in the upper layer to be nearly orthogonal to the wind (Lacomb et al. 1972). In shallow water, where drift

Corresponding author address: Professor V. A. Sukhorukov, Computing Centre, Siberian Division of the USSR, Academy of Sciences, Novosibirsk 630090, USSR.

currents may reach to the bottom, the phenomenon of current velocity turning towards the wind and the presence of a constant friction stress layer are to be expected. To study these phenomena by mathematical modeling, turbulence exchange models should be used.

The physical processes taking place in the upper mixed layer (UML) of the ocean are diverse. The UML is basically formed by small-scale turbulence brought about by the breaking of surface waves, by shear instability of inertial and drift currents, and by thermal and thermohaline convection arising when cooling or evaporation from the ocean surface occurs. Internal waves cause microstructure formations and can transfer energy from the mixed layer to a thermocline. The stabilizing factors are the dissipation of small-scale fluctuations and the work by buoyancy forces in converting kinetic energy of turbulence to potential energy. Langmuir circulation produces effective heat transport from the surface to the lower boundary of the UML.

Models applied in determining the turbulence exchange in the UML are based on correlation equations. As a rule, in these models there is no correlation between surface waves and small-scale turbulence. Therefore, when solving such models, the upper boundary is chosen as deeper than the free surface. The frictional wind stress, transformed by the breaking of short surface waves, produces drift currents and creates a small-scale turbulence flux into the ocean. There is a point of view that the impact of the breaking surface wave is concentrated in the upper several meters, while the small-scale turbulence is caused by the velocity shear in the UML (Oakey and Elliot 1980). According to another point of view, wave turbulence penetrates much deeper, ten times deeper than the surface wave height (Kitaigorodsky et al. 1983). There are assumptions that in the upper layer the velocity profile is described by the logarithmic law, which agrees with laboratory and in situ measurements (Kondo 1976). The fact that the logarithmic velocity law really exists in the bottom boundary layer is proven by experiments (Kullenberg and Zaneveld 1983). Later we will consider theoretically the logarithmic velocity profile for shallow water.

The existing models of small-scale ocean turbulence are based on correlation equations and differ principally in the equation for the turbulence scale or its analogues; for example, see Mellor and Durbin (1975) and Marchuk et al. (1977). A detailed survey of turbulence models currently applied is given by Rodi (1987).

The idea of constructing the hierarchy of turbulence models for the planetary boundary layer of the atmosphere (Mellor and Yamada 1974) can be extended to the UML of the ocean in more than one way. Let us look at one such approach based on the VTE coefficient concept where two energetic equations of turbulence are suggested as equations of small-scale ocean turbulence dynamics. They are those of turbulence kinetic energy (TKE) and dissipation of turbulence kinetic energy (DTKE) (*Kochergin et al. 1974*). In the paper by Kochergin et al. (1977) the model is simplified; the substantiation of the generalized Prandtl formula is given by $K = L^2(U^2 + V^2 - g\rho_z/\rho_0)^{1/2}$, in which the mixing length, L, is determined from the mixed layer thickness, h. Energetic turbulence equations (ETE) are proposed to study the laws (similar to the laws of the atmospheric boundary layer) of the drift friction layer of the ocean formation when fine numerical vertical resolution is required. This is especially true of UML deepening in a storm when a local boundary layer with the extremum of DTKE may occur at the UML base (Marchuk et al. 1977). Oakey and Elliot (1980) emphasized this when analyzing in situ measurements. It would be reasonable to apply the Prandtl formula to the problems with a rough spatial resolution such as those of the general circulation of the ocean (Marchuk et al. 1978; Sunderman et al. 1983; Sukhorukov and Tausnev 1986). The next step in the modeling hierarchy is the analytical theory formed in elementary functions for the stationary turbulent drift friction layer of the ocean (Sukhorukov and Dmitriev 1986). These methods of modeling the UML were checked against the data of the FLEX experiment (Friedrich et al. 1981; Kazakov and Sukhorukov 1984) and those taken from the ocean weather station "C" (Sukhorukov et al. 1986). Prognostic numerical experiments were carried out for a period of two months using an approximation of the equations of the horizontally homogeneous boundary layer. They demonstrated that in spring and summer all three methods reproduce turbulence characteristics in a similar manner in the upper layer of the ocean. Therefore, in practice it's better to use the generalized Prandtl formula and, if we neglect the nonstationary state, to employ analytical formulae. Spectral analyses of the simulated drift velocity fields from the FLEX experiment made it clear that the main contribution to kinetic energy is made by inertial oscillations whose relative contribution increases with depth. Short-wave atmospheric perturbations are filtered out in the upper layer and long periods, such as synoptic variations of wind velocity with depth, manifests itself in a modulation of the velocity field associated with inertial oscillations (Sukhorukov 1985). Anderson et al. (1983) provide an experimental verification of such phenomena.

The present paper puts forward the theory of a stationary drift friction layer of the ocean, which may appear as an UML in the deep ocean or a layer mixed from surface to the bottom in shallow water under the conditions of stable stratification.

2. Analytical solutions of drift current equations

Let us look at a stationary DCE:

$$(KW_z)_z - ifW = 0. \qquad (1)$$

Here $W = U + iV$; U, V are the horizontal velocity component, z is the vertical downward component, f

is the Coriolis parameter, $i = \sqrt{-1}$. Coefficient K is assumed to be zero at the boundary $z = H$. Therefore, in this case, instead of a boundary condition at this point, we require the solution to be bounded:

$$z = 0: KW_z = -u_*^2; \quad z = H: |W| < \infty, \quad (2)$$

where u_* is the dynamic velocity in the wind direction.

Any analytic function can be expanded in an infinite power series. Consider the solution of Eq. (1) with the coefficient $K(z)$ represented in the form of a power series

$$K(x) = (1 - x)^m \sum_{n=0}^{\infty} a_n(1 - x)^n, \quad x = z/H, \quad m \geq 0. \quad (3)$$

We assume that $a_0 \neq 0$, $K(x) \geq 0$, and the coefficient K is not zero anywhere within the interval (0, 1), except for possibly the point $x = 1$. Then for $m \leq 2$, the Fuchs theorem is valid for Eq. (1) (Tricomi 1962) and the solution can be found from the power series (Sukhorukov and Dmitriev 1983).

For $m = 2$ the solution takes the form:

$$W(x) = \frac{u_*^2 H}{K_0}(1 - x)^{\omega} \frac{\sum_{j=0}^{\infty} c_j(1 - x)^j}{\sum_{j=0}^{\infty} c_j(j + \omega)}, \quad (4)$$

where $K_0 = K(0)$, $\omega = M + iN$, $A = 8(\pi H/D)^2$, $D = \pi\sqrt{2K_0/f}$,

$$M = \frac{1}{2}\left\{\left[\frac{1}{2}(1 + A^2)^{1/2} + 1\right]^{1/2} - 1\right\},$$

$$N = \frac{1}{2}\left[\frac{1}{2}(1 + A^2)^{1/2} - 1\right],$$

and the coefficients c_j are found from the recursion formula

$$c_0 = 1, \quad (2\omega + 1 + j)jc_j = -(\omega + 1 + j)\sum_{k=0}^{j-1} c_k \times (k + \omega)(a_{j-k}/a_0), \quad j = 1, 2, \cdots.$$

The presence of the factor $(1 - x)^{iN} = \exp[iN \ln(1 - x)]$ in the solution causes the infinite number of turns of the velocity vector at $x \to 1$ (Kozlov 1963). Investigating the dependence of W_x in the vicinity of $x = 1$ on the dimensionless relation H/D (where D is depth of the Ekman friction layer determined above), it can be shown that if $H/D < E = \pi^{-1}(1.5\sqrt{2})^{1/2} \approx 0.46$, $W_x \to \infty$; if $H/D > E$, $W_x \to 0$; and if $H/D = E$, $W_x = \text{const}$. Consequently, if $H/D < E$, the spiral of the velocity hodograph has explicitly noticeable rotation in the vicinity of the point $x = 1$. An example of this rotation is given in Sukhorukov and Dmitriev (1983). This mathematical effect of a singular problem has no physical analogue. When K is allowed to be nonzero at the boundary H, this effect vanishes.

For $m = 1$ the solution takes the form:

$$W(x) = \frac{u_*^2 H}{K_0}\sum_{j=0}^{\infty} c_j(1 - x)^j \Big/ \sum_{j=0}^{\infty} jc_j, \quad (5)$$

$$c_0 = 1, \quad c_1 = ifH^2/a_0,$$

$$jc_j = -ifH^2 c_{j-1}/a_0 - j\sum_{k=0}^{j-2} c_{k+1}(k + 1)(a_{j-k-1}/a_0), \quad j = 2, 3, \cdots.$$

Let us consider the asymptotic properties of the solution for $H/D \to 0$. We will obtain

$$W(x) = -iu_*^2/(fH),$$

i.e., for sufficiently small values of the magnitude H/D, the velocity vector tends to turn normal to the wind direction in the whole layer $[0, H]$. Note that at the point $x = 1$, velocities do not vanish, however, they tend to zero, as the ratio H/D increases.

For $m = 0[K(x) > 0]$ consider asymptotic properties of the two solutions with different boundary conditions. The solution with the boundary condition $W = 0$ at $x = 1$ will be

$$W(x) = \frac{u_*^2 H}{K_0}(1 - x)\frac{\sum_{j=0}^{\infty} c_j(1 - x)^j}{\sum_{j=0}^{\infty} c_j(j + 1)}, \quad (6)$$

$$KW_x = -u_*^2 H\sum_{j=0}^{\infty} a_j(1 - x)^j \frac{\sum_{j=0}^{\infty} c_j(1 + j)(1 - x)^j}{\sum_{j=0}^{\infty} c_j(j + 1)}, \quad (7)$$

$$c_0 = 1, \quad c_1 = -a_1/(2a_0), \quad (D = \pi\sqrt{2K_0/f}),$$

$$j(1 + j)c_j = ifH^2 c_{j-2}/a_0 - j\sum_{k=0}^{j-1} c_{k+1}(k + 1) \times (a_{j-k}/a_0), \quad j = 2, 3, \cdots.$$

In the vicinity of the boundary $x = 1$, one can distinguish the domain where the velocity has a linear profile, here the profile of the coefficient K determines only the slope. When the H/D_H and a_j/a_0 ratios decrease, the solution tends to the linear profile in the whole layer of depth H.

$$W(x) \to \frac{u_*^2 H}{K_0}(1 - x).$$

With the depth H decreasing or the coefficient a_0 increasing, (the boundedness of the ratio $a_j/a_0 (a_j/a_0 < \infty)$ being necessary in the latter case), the current

in the whole layer deviates from the wind direction to a lesser extent, since the coefficients c_j become real as $H/D_H \to 0$. Here $D_H = \pi\sqrt{2K_H/f}$ is the depth of the friction layer determined by the coefficient K_H.

Let us next look upon the behavior of the friction stress components. Formula (7) reduces to

$$KW_x = -u_*^2 H \frac{1 + ifH^2 \sum_{j=0}^{\infty} \frac{1}{j+2} c_j (1-x)^{j+2}}{1 + ifH^2 \sum_{j=0}^{\infty} \frac{1}{j+2} c_j}. \quad (8)$$

In the vicinity of $x = 1$ one can distinguish the domain where the friction stress can be considered constant.

$$KW_z \approx \frac{u_*^2}{\sum_{j=0}^{\infty} c_j (j+1)} \frac{K_H}{K_0}.$$

As the depth H decreases or the coefficient a_0 increases and the ratios a_j/a_0 are bounded, the domain of constant friction stresses grows since, as $H/D_H \to 0$, we have $KW_z \to u_*^2$ in the whole domain $[0, H]$. The change in the friction stress with respect to depth becomes marked when $0.5fH^2(1-x)^2/a_0 \approx 1$. Hence the domain of the constant stress can be estimated as follows:

$$h_{\text{const}} \approx \sqrt{2K_H/f} = D_H/\pi.$$

Let us assume that the coefficient $K(x)$ is linearly dependent on x, of the form $K(x) = a_0 + a_1(1-x)$, then the solution may appear as

$$|W(x)| = \frac{u_*^2 H}{a_0} \left\{ \frac{\ln^2\left[1 + \frac{a_1}{a_0}(1-x)\right] + E_H^2 \sum_{n=0}^{\infty} \xi_n \left(\frac{a_1}{a_0}\right)^n (1-x)^n}{1 + E_H^2 \sum_{n=3}^{\infty} \xi_j (a_1/a_0)^n} \right\}^{1/2},$$

if the condition $(a_j/a_0)(1-x) < 1$ is satisfied, under which the expansion of $\ln[1 + (a_1/a_0)(1-x)]$ in a power series is valid. If $a_j/a_0 < 1$, the solution holds for all the domain $[0, 1]$. Sufficient conditions to distinguish the logarithmic velocity profile in the domain $[0, 1]$ are $E_H = (\pi H/D_H)^2 < 1$ and $a_j/a_0 < 1$, then

$$|W(x)| \to (u_*^2 H/a_0) \ln[1 + (a_1/a_0)(1-x)].$$

If we assume $K(z) = \kappa z_0 u_* + \kappa u_*(H - z)$, where κ is the traditional von Kármán constant and z_0 is the roughness length, we obtain

$$|W(x)| \to (u_*^2 H/\kappa z_0) \ln[1 + (H/z_0)(1 - z/H)].$$

Sufficient conditions $E_H = H^2 f/(2\kappa z_0 u_*) < 1$ and $a_1/a_0 = H/z_0 < 1$ indicate that the logarithmic profile is possible in very shallow water. In this case, presumably, the constant profile of the coefficient $K(z)$ is preferable, and hence the linear velocity profile, the first term of the logarithmic expansion in a series. If the condition $H/z_0 < 1$ is not fulfilled, $H/z_0 < 1$, then strictly speaking, the logarithmic profile domain in the vicinity $x = 1$ will not exceed $(1-x) < z_0/H$, where the linear number may again prove to be dominant.

Consider the solution satisfying the boundary condition $KW_x = 0$ at $x = 1$.

$$W(x) = \frac{u_*^2 H \sum_{j=0}^{\infty} d_j (1-x)^j}{K_0 \sum_{j=0}^{\infty} d_{j+1}(j+1)}, \quad (9)$$

$$KW_x = -u_*^2 H (1-x) \sum_{j=0}^{\infty} a_j \times (1-x)^j \frac{\sum_{j=0}^{\infty} d_{j+2}(2+j)(1-x)^j}{\sum_{j=0}^{\infty} d_{j+2}(j+2)}, \quad (10)$$

$$d_0 = 1, \quad d_1 = 0, \quad j(1+j)d_j = ifH^2 d_{j-1}/a_0 - j \sum_{k=0}^{j} d_k k \left(\frac{a_{j-k+2}}{a_0}\right), \quad j = 2, 3, \cdots.$$

With the depth H decreasing or the coefficient a_0 increasing and the relations a_j/a_0 being bounded, the current velocity vector tends to turn normal to the wind direction. It follows from (9) and the fact that the coefficients d_j go to zero provided that $H/D_H \to 0$. From (10) it follows that in the vicinity of the boundary $x = 1$, there can be distinguished the domain where the friction stress has a linear profile. As it takes place, with the depth H decreasing or the coefficient a_0 increasing, the ratio a_j/a_0 being bounded, the friction stress components tend to a linear distribution throughout the domain with the depth H.

The analysis carried out of the solutions of drift current equations (DCE) makes it possible to formulate the following conclusions. Let the VTE coefficient be an analytical function vanishing nowhere in the domain $[0, H]$, then the following theorems hold for the solutions of equations of the ocean drift currents.

Theorem 1. If the boundary condition $KW_x = 0$ is fulfilled at $z = H$, then in the vicinity of this boundary one can always distinguish the domain with linear distribution of the friction stress components. And when the depth H decreases or the coefficient K_H ($K_H = a_0$) increases, with the ratio a_j/a_0 being bounded, in the whole layer with the depth H, drift velocities tend to

turn at an angle of $\pi/2$ to the wind direction and friction stress components tend to linear distribution.

Theorem 2. If the boundary condition $W = 0$ holds at $z = H$, then in the vicinity of this boundary one can always distinguish the domain with constant values of the friction stress components. Furthermore, as depth H decreases or the coefficient K_H increases, the relations a_j/a_0 being bounded, the drift velocities throughout the layer with depth H tend to turn towards the wind direction and the friction stress components tend to constant distribution.

Theorem 3. If the boundary condition $W = 0$ is satisfied at $z = H$, then in the vicinity of this point one can always distinguish the domain where velocity is linear. With the ratios H/D_H and a_j/a_0 decreasing this vicinity broadens and, in the limit, it tends to the whole domain $[0, H]$.

For the coefficient $K(z)$ of a power form based on the solutions obtained by Kozlov (1963) and Dmitriev and Sukhorukov (1982) we will formulate the following assertion.

Assertion. If the coefficient $K(z)$ has the form $K = K_0(1 - z/H)^n$, $n \geq 2$, then as the depth H increases, the velocity value at the surface tends to Ekman's classical solution (Kozlov 1963; Dmitriev and Sukhorukov 1982). As this takes place, the conditions $W = 0$ and $KW_z = 0$ are simultaneously valid at $z = H$ (Sukhorukov and Dmitriev 1984).

The analysis of numerical solutions of the DCE with the coefficient $K(z)$ of a power form with the exponent n, $0 \leq n < 2$, shows that the assertion is valid at any $n \geq 0$ (when $n < 2$, the boundary condition $W = 0$ or $KW_z = 0$ is satisfied).

Let us illustrate theorems 1, 2 by some particular examples. Figures 1, 2 display profiles of friction stress components, velocity module and the angle of the velocity vector rotation for the two types of the coefficient $K(x)$ which provide the solutions of the turbulence model equations and experimental estimates.

Figure 1 is an illustration of Theorem 1. In the vicinity of the boundary $x = 1$, the linear domain can be distinguished in the profiles of friction stress components KU_x, KV_x and with H decreasing ($H/D = 1$, 0.5, 0.25) the domain increases, reaching the surface $z = 0$, while the velocity vector of drift currents tends to turn at an angle of $\pi/2$ to the wind direction.

Figure 2 illustrates Theorem 2. As the depth H decreases, ($H/D = 1, 0.5, 0.25, 0.125$), the drift currents in the whole domain $[0, H]$ tend to turn towards the wind direction and the layer of constant friction stresses is formed, $KU_z = -u_*^2$, $KV_z = 0$.

In both cases an increase in convexity of the coefficient $K(z)$ makes the assertion formulated in Theorems 1, 2 more precise. Diagrams shown in Figs. 1, 2 are plotted when the external parameters have the following values: $K_0 = 50\ \text{cm}^2\,\text{s}^{-1}$, $f = 10^{-4}\ \text{s}^{-1}$, $K_H = 1\ \text{cm}^2\,\text{s}^{-1}$, $u_* = 1\ \text{cm}\,\text{s}^{-1}$. The velocity module and friction stress components are presented in dimensionless form with respect to the velocity u_*. The properties of drift currents stated in Theorems 1, 2 become more distinct if the condition $H/D < 1$ holds.

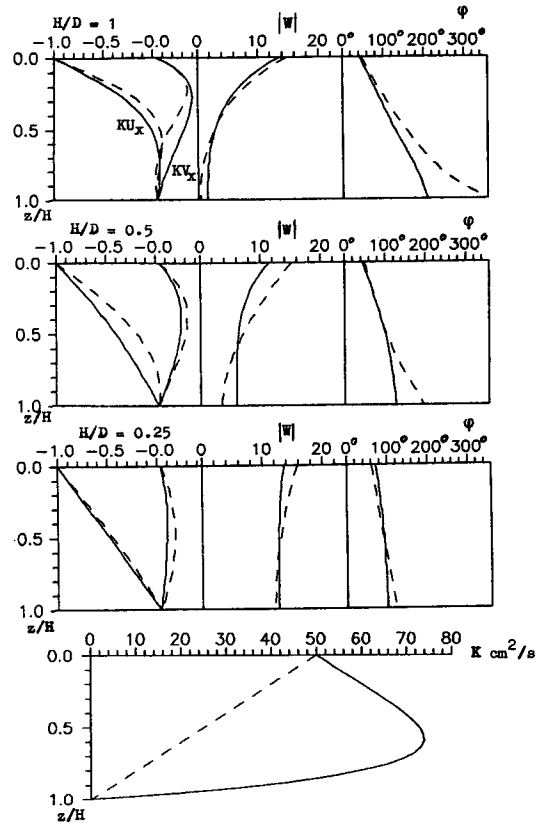

FIG. 1. Profiles of values KU_z, KV_z, $|W(z)|$, $\varphi(z)$ for the respective profiles of the coefficient K, $KW_z(z = H) = 0$.

Figure 3 illustrates the display of the logarithmic velocity profile for a linear profile $K(z)$ in the realistic physical domain with the bottom coefficient K_H increasing.

3. VTE model

Dimensionless ratios H/D and H/D_H are the key parameters in the above theorems. The question arises as to the factors causing the change in these parameters. The regime stated in Theorem 2 is, presumably, found in shallow water where drift currents reach to the bottom. Observation of drift currents in summer under the conditions of stable stratification report on the absence of friction stress at the UML base (Lacombe et al. 1972). Therefore the regime stated in Theorem 1 should be sought for in the UML when shallowing.

To simulate the conditions mentioned, we examine turbulence energy equations for the determination of the coefficient $K(z)$ (Kochergin et al. 1974; Marchuk et al. 1977).

$$KW_zW_z^* + (Kb_z)_z - \epsilon - \mu u_*^3/\lambda = 0, \quad (11)$$

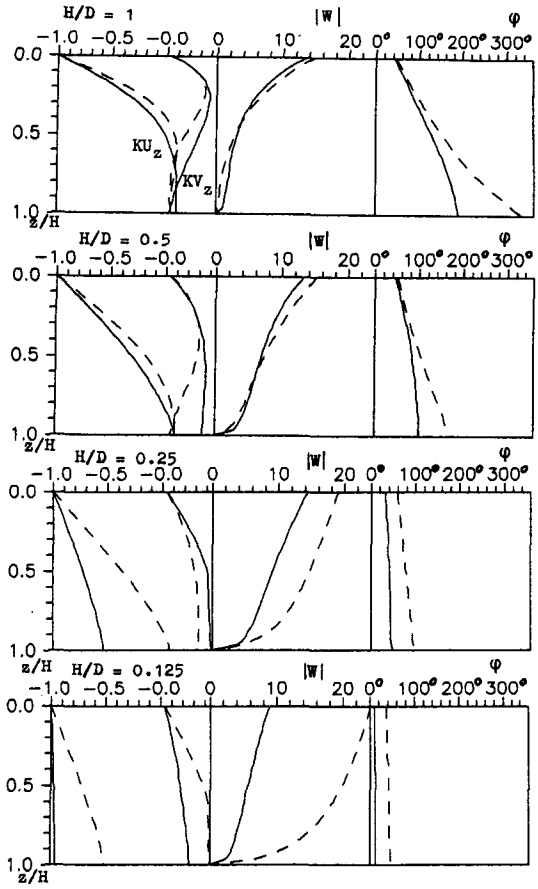

FIG. 2. Profiles of values KU_z, KV_z, $|W(z)|$, $\varphi(z)$ for the respective profiles of the coefficient K, illustrated in Fig. 1, $W(z = H) = 0$.

$$c_{1\epsilon}\frac{\epsilon}{b}KW_zW_z^* + (K\epsilon_z)_z - c_{2\epsilon}\frac{\epsilon}{b}\epsilon - c_{3\epsilon}\frac{\epsilon}{b}\mu u_*^3/\lambda = 0, \tag{12}$$

$$K = c_\mu b^2/\epsilon, \tag{13}$$

$$z = 0: Kb_z = 0, \quad K\epsilon_z = 0; \quad z = H: b = 0, \quad \epsilon = 0, \tag{14}$$

or

$$z = H: b_z = 0, \quad \epsilon = KW_zW_z^* + (Kb_z)_z - \mu u_*^3/\lambda. \tag{15}$$

Here b is the TKE, ϵ is the dissipation rate of turbulent kinetic energy (DTKE), $\mu = g\alpha Q\lambda/u_*$ is the dimensionless stratification parameter, $\lambda = u_*/f$ is the length scale, $g\alpha$ is the buoyancy parameter and Q is the heat flux normalized with respect to density and specific heat, $W^* = U - iV$.

Based on the formulated problem (11)–(15) and (1) and (2), we investigate the effect of stratification and boundary conditions $W = 0$ or $KW_z = 0$ at $z = H$ on the formation of the drift friction layer. The technique of solving this system is described in Kochergin and Sukhorukov (1975). The problems corresponding to these boundary conditions were numerically calculated and analyzed. The constants in the ETE model are assumed as follows: $c_{1\epsilon} = 1.38$, $c_{2\epsilon} = 1.4$, $c_{3\epsilon} = 1.4$, $c_\mu = 0.08$.

The variants for the six values of the dimensionless parameter of stratification μ (see Table 1) were numerically calculated for the case when the boundary condition $KW_z = 0$. A uniform grid with mesh size from 5 cm (for $\mu = 100$) to 30 cm (for $\mu = 0.01$) was used. The depth H was taken deeper than h so that boundary conditions (14) at $z = H$ had no effect on characteristics of the turbulent layer. The depth of the surface turbulent layer h was determined as the first point of the calculated grid, at which the condition $K(z) \leqslant K_h$ was satisfied. φ_0 denotes the value of the rotation angle of the velocity vector at the surface relative to the wind direction. The values of the outer parameters are taken as follows: $u_* = 1$ cm s^{-1}, $f = 10^{-4}$ s^{-1}, $g\alpha Q = (10^{-6}/10^{-2})$ cm^2 s^{-3}, $K_h = 1$ cm^2 s^{-1}.

Since the coefficient K varies in the surface turbulent layer with the depth h, the ratio h/D is the analogue

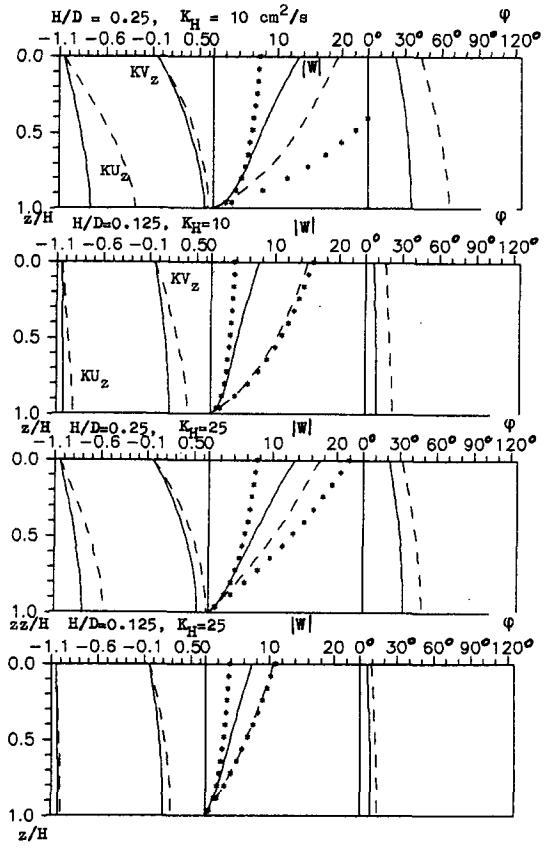

FIG. 3. Profiles of values KU_z, KV_z, $|W(z)|$, $\varphi(z)$ for the respective profiles of the coefficient K, illustrated in Fig. 1, $W(z = H) = 0$. The velocity $|W(z)|$ calculated by logarithmic formula is marked with points.

TABLE 1. Calculated hydrodynamic values at different values of the parameter μ.

μ	0.01	0.1	1.	10.	50.	100.
h/D	0.70	0.63	0.48	0.28	0.18	0.14
φ_0 (deg)	50.3	50.3	50.3	59.7	68.1	69.7
$\lvert W_0\rvert$ (cm s^{-1})	7.06	7.06	7.15	10.3	18.3	24.7
K_0 (cm^2 s^{-1})	223	221	214	108	53	38
b_0 (cm^2 s^{-2})	3.00	3.00	2.97	2.48	2.45	2.11
ϵ_0 ($\times 10^{-3}$) (cm^2 s^{-3})	3.24	3.25	3.29	6.0	9.1	9.3
h (cm)	4650	4175	3120	1280	585	396
$\lvert KW_z\rvert_{z=h}/u_*^2$ (%)	0.1	0.3	1	4	10	14
$\epsilon_I/(u_0u_*^2)$ (%)	100	100	93	75	57	53
$g\alpha Qh/(u_0u_*^2)$ (%)	0	0	7	25	43	47
$\epsilon_I/(U_{10}u_*^2)$ (%)	0.56	0.56	0.53	0.48	0.48	0.57

of the dimensionless ratio H/D. Numerical solutions show that an increase in the parameter μ results in a decrease in the ratio h/D. In the vicinity of the point $z = h$ the condition $KW_z = 0$ holds with high accuracy and is necessary for the phenomena stated in Theorem 1. Note that in these calculations boundary condition $W = 0$ (14) is used at $z = H$. With μ increasing, the magnitudes h, K_0, b_0 decrease and the values of the magnitudes φ_0, $|W_0|$, ϵ_0 become larger. Note that numerical solutions asymptotically approach the neutral-stratification solution when the value $\mu \approx 1$ and that further decrease of the parameter μ does not alter hydrodynamic and turbulent characteristics in the domain of the solutions except for the vicinity $z = h$. The profile of the coefficient $K(z)$ approaches the shape of the universal curve and the angle φ_0 is greater than 45°, $\varphi_0 = 50°$. A similar effect was pointed out by Kundu (1980a). These results may contribute to an explanation of why the classical Ekman spiral does not come about in nature under stable stratification conditions. Figures 4, 5 present the profiles $K(z)$, $|W(z)|$, $\varphi(z)$ and the balance of the terms of the TKE equations only for the three values of μ, $\mu = 1$, 10, 100 denoted by numbers 4, 5, 6, respectively. Generation and dissipation are the basic terms in the balance of the TKE equation. The contribution of the diffusion term is much smaller.

Table 1 gives the integral balance of terms of the TKE equations ϵ_I ($\epsilon_I = \int_0^h \epsilon dz$) and $g\alpha Qh$ relative to the kinetic energy flux in the ocean $u_*^2 u_0(\tau \mathbf{V}_0)$ and in the atmosphere $u_*^2 U_{10}$ ($\rho_a u_*^2 U_{10} = C_d \rho_a U_{10}^2 U_{10}$, $C_d = 1.3 \times 10^{-3}$, $\rho_a = 1.2$ kg m^{-3}). In the balance, dissipation dominates over the work of Archimedean buoyancy forces. Oakey (1985) reports on experimental estimates of the ratio $\epsilon_I/(U_{10}u_*^2)$ taking up 0.4% in the JASIN experiment and 1.2% in Emerald Basin. Our values agree better with the JASIN data.

Let us now consider the solutions applicable to the shallow conditions where drift currents extend to the bottom. Here we mean solutions obtained when the stratification parameter $\mu = 1$ and the depths of domain H are equal to 10, 15, 20 meters labeled in Figs. 4, 5 by 1, 2, 3, respectively, because according to the earlier numerical experiments, at $\mu = 1$ the depth of the turbulent layer h is 30 meters. Here we examine the role of the boundary conditions $W = 0$ at $z = H$. Conditions (15) are assigned as boundary conditions for energetic turbulent equations, similar to the conditions in the constant flux layer near a solid wall. Calculations show that a decrease in the depth H results in the rotation of the velocity towards the wind direction, the velocity amplitude being linear. TKE generation of $KW_zW_z^*$ becomes constant in this domain as well (Fig. 5). The contribution of the diffusion term $(Kb_z)_z$ in the balance of the TKE equation is insignificant, hence the dissipation ϵ (Fig. 5) and the TKE b are constant, too.

Calculations demonstrate the $K(z)$ coefficient to become constant in all the domain; i.e., the coefficients of its expansion in a power series a_1, a_2, a_3, ... tend to zero. In this case, it follows from theorem 3 that as the dimensionless parameter H/D_H decreases, the domain of the linear velocity profile increases at a rate

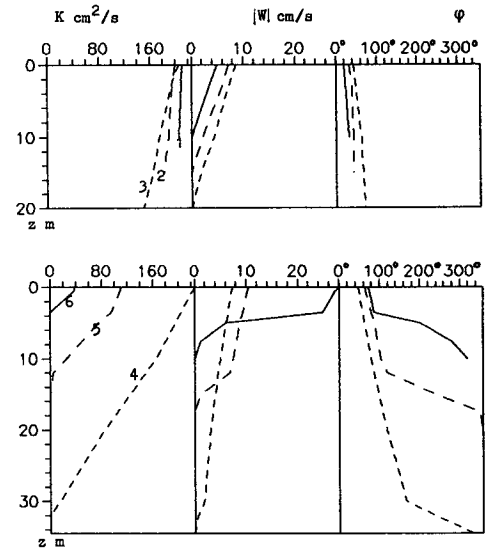

FIG. 4. Profiles of the coefficient K, dimensionless amplitude of the velocity vector $W(z)$ and turning angle of velocity vector $\varphi(z)$: (a) solution for shallow water condition at $\mu = 1$, $H = 10$, 15, 20 meters are marked 1, 2, 3; (b) solution for UML at $\mu = 1$, 10, 100 by 4, 5, 6.

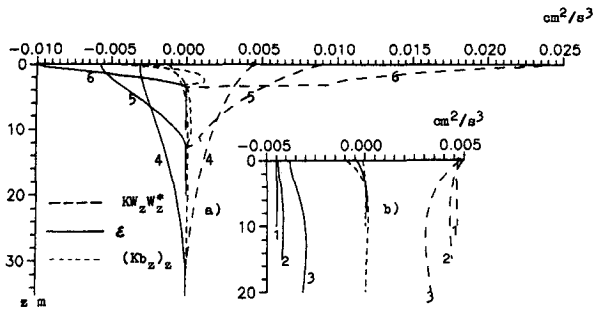

FIG. 5. Balance of TKE equation terms (without $g\alpha Q$) for the UML conditions (a) and for the shallow water (b). Variants are labeled in the same way as Fig. 4.

being determined by the ratio $(H/D_H)^2$. This may come about as the depth H decreases or as the scale D_H becomes larger, which are observed in Fig. 4. These results may be formulated as a corollary of Theorems 2, 3.

Corollary. When the conditions of Theorem 3 are satisfied, the conditions of Theorem 2 are valid as well. In this case the velocity profile is linear in the layer of constant stress, therefore the VTE coefficient in the layer of constant stress becomes constant, consequently the generation source $KW_zW_z^*$ in the TKE equation is constant.

Our, to an extent idealized, calculations show that a linear velocity profile may form in a shallow water and the turbulence parameters K, b, ϵ, $KW_zW_z^*$ and the friction stress become constant, independent of the vertical coordinate.

4. Analytic models for the turbulent drift friction layer of the ocean

Let us construct analytical models of the turbulent drift friction layer both for a deep ocean and shallow water. Numerical solutions of problems (1), (2), (11)–(15) have shown the turbulent diffusion in the balance of the terms in TKE to be substantially less than the other terms. With this assumption in mind, Eq. (11) can be written in the form:

$$G - \epsilon - \mu u_*^3/\lambda = 0, \quad G = KW_zW_z^*. \tag{16}$$

Let us introduce the function of dimensionless parameters of the problem $\Phi_1(\mu)$

$$\epsilon_0/G_0 = 1 - \Phi_1(\mu), \tag{17}$$

where ϵ_0, G_0 are values of the functions at $z = 0$. Using boundary condition (2), that $G_0 = u_*^4/K_0$, and Eqs. (16), (17), we arrive at

$$K_0 = \frac{u_*\lambda}{\mu}\Phi_1(\mu), \quad G_0 = \frac{u_*^3}{\lambda}\frac{\mu}{\Phi_1(\mu)},$$

$$\epsilon_0 = \frac{u_*^3}{\lambda}\frac{\mu}{\Phi_1(\mu)}(1 - \Phi_1(\mu)),$$

$$b_0 = 2.5\sqrt{2}u_*^2(1 - \Phi_1(\mu))^{1/2}. \tag{18}$$

To determine the other turbulent magnitudes let us use the technique suggested by Marchuk et al. (1979) and Sukhorukov and Dmitriev (1984). Assume that the coefficient K has a power form:

$$K = K_0(1 - z/H)^n = K_0(1 - x)^n,$$

$$n \geqslant 0, \quad x = z/H.$$

For integer positive n the solution of Eq. (1) in elementary functions exists only for three values of n ($n = 0, 2, 4$) (Kozlov 1963).

Let us consider the case when $n = 4$. The solution of equation (1) with boundary condition (2) takes the form (Dmitriev and Sukhorukov 1982):

$$U, V = \frac{u_*^2}{fH}\frac{\sqrt{\beta^2 + (1 - x + \beta)^2}}{(1 - x)} \times \exp(-\beta x/(1 - x))[\cos\psi, \sin\psi],$$

$$\beta = \pi H/D, \ \psi(x) = \beta x/(1 - x) - \tan^{-1}[1 + (1 - x)/\beta].$$

Let us determine the boundary of the surface turbulent layer h as a point at which the VTE coefficient K is equal to the a priori fixed value K_h, $K_h = K(h)$. Let us introduce a function of dimensionless parameters, $\Phi_2(\mu)$, by analogy with $\Phi_1(\mu)$

$$\epsilon_h/G_h = 1 - \Phi_2(\mu). \tag{19}$$

By this equality and expressions (16)–(18) we find the basic characteristics of the problem:

$$H = \lambda\beta\left(\frac{2\Phi_1}{\mu}\right)^{1/2},$$

$$h = \lambda\left(\frac{\Phi_1}{4\mu\ \mathrm{Re}_h}\right)^{1/4}\ln\left[\frac{\Phi_1}{\Phi_2}\left(\frac{\Phi_1\ \mathrm{Re}_h}{\mu}\right)\right]^{1/2},$$

$$\epsilon = \frac{u_*^3}{\lambda}\frac{\mu}{\Phi_1(\mu)} \times \{(1 - x)^{-2}\exp[-2\beta x/(1 - x)] - \Phi_1(\mu)\},$$

$$b = 2.5\sqrt{2}u_*^2(1 - x)^2 \times \{(1 - x)^{-2}\exp[-2\beta x/(1 - x)] - \Phi_1(\mu)\}^{1/2},$$

$$\beta = 0.5\frac{\ln[(\Phi_1/\Phi_2)(\Phi_1\ \mathrm{Re}_h/\mu)^{1/2}]}{(\Phi_1\ \mathrm{Re}_h/\mu)^{1/4} - 1},$$

$$x = \frac{z}{\lambda}\frac{1}{\beta}\left(\frac{\mu}{2\Phi_1}\right)^{1/2},$$

where $\mathrm{Re}_h = u_*\lambda/K_h$.

Similarly we can obtain the solution for the coefficients K of the form: $K = \mathrm{const}$, $K = K_0[1 - (z - z_0)^2/(H - z_0)^2]$, $K = K_0(1 - z/H)^2$ (Sukhorukov and Dmitriev 1984).

The functions Φ_1, Φ_2 are selected on the basis of numerical solutions of section 3. Asymptotic Φ_1 of the parameter μ has the form $\Phi_1 \to 0$ for $\mu \to 0$, which

follows from Eqs. (16): $G_0 \to \epsilon_0$, and $\Phi_1 \to 1$ for $\mu \to \infty$ which follows from the numerical solutions. One of the possible functions that meets the requirements stated will be

$$\Phi_1 = \mu/(\mu + c_1), \quad c_1 = 45,$$

where c_1 is selected so that K_0 coincides with the numerical solution for $\mu \approx 0$.

Before determining the function Φ_2 it should be noted that this function is used in the solution in the ratio $\Phi_1/\Phi_2 = G_h/G_0$ only. The asymptote of the ratio can be determined from the numerical solution analysis and general considerations

$$\Phi_1/\Phi_2 = G_h/G_0 = \begin{cases} \text{const}, & \mu \to 0 \\ 1, & \mu \to \infty. \end{cases}$$

By analogy with the function Φ_1 the function Φ_2 is constructed

$$\Phi_2 = \mu/(\mu + c_2).$$

The constant c_2 is determined from the condition that in a neutral-stratificated medium it is usually assumed that $\gamma_0 = h/\lambda \approx 0.4$. Hence we obtain

$$c_2 = \sqrt{c_1 \operatorname{Re}_h} \exp[-\gamma_0(4c_1 \operatorname{Re}_h)^{1/4}].$$

These solutions are applicable to the stationary stably stratified UML of the ocean. Let us now consider the solution applicable to shallow water. The coefficient K is then assumed constant and $W = 0$ at the $z = H$. Reasoning in a similar way we arrive at the following

$$K = u_* \lambda(\mu_1 + c_1)^{-1}, \tag{20}$$

$$|W| = u_*[(\mu + c_1)F(x)]^{1/2},$$

$$\varphi = \tan^{-1}[\tan(\beta(1-x))\operatorname{cotanh}(\beta(1-x))] - \tan^{-1}[\tan\beta \tanh\beta] - \pi/4,$$

$$\epsilon = \frac{u_*^3}{\lambda}(\mu + c_1)\left[F(x) - \frac{\mu}{\mu + c_1}\right],$$

$$b = 2.5\sqrt{2}u_*^2\left[F(x) - \frac{\mu}{\mu + c_1}\right]^{1/2},$$

$$\beta = \pi\sqrt{0.5(\mu + c_1)}\,H/\lambda,$$

$$F(x) = \frac{\cos^2(\beta(1-x))\sinh^2(\beta(1-x)) + \sin^2(\beta(1-x))\cosh^2(\beta(1-x))}{\cos^2\beta\cosh^2\beta + \sin^2\beta\sinh^2\beta}.$$

To make the analysis more convenient, let us also present the solutions for the case when $K = K_0(1-x)^2$ is applicable to the UML of the ocean:

$$K = u_* \lambda(\mu_1 + c_1)^{-1}(1-x)^2,$$

$$|W| = u_*\beta[2(\mu + c_1)/(2m^2 + m)]^{1/2}(1-x)^m,$$

$$\varphi = \tan^{-1}(1 + 1/m)^{1/2} - (m^2 + m)^{1/2}\ln(1-x),$$

$$H = \lambda\beta[2/(\mu + c_1)]^{1/2},$$

$$\gamma = h/\lambda = \sqrt{2}\beta[(\mu + c_1)^{-1/2} - \operatorname{Re}_h^{-1/2}],$$

$$\epsilon = u_*^3\lambda^{-1}(\mu + c_1)[(1-x)^{2m} - \mu(\mu + c_1)^{-1}],$$

$$b = 2.5\sqrt{2}u_*^2(1-x)[(1-x)^{2m} - \mu(\mu + c_1)^{-1}]^{1/2},$$

$$\beta = \pi H/D = 0.25\sqrt{2}\{[2(2m+1)^2 - 1]^2 - 1\}^{1/4},$$

$$m = \ln[(\mu + c_1)(\mu + c_2)^{-1}]/\ln[\operatorname{Re}_h(\mu + c_1)^{-1}],$$

$$c_2 = c_1^{1+m_0}\operatorname{Re}_h^{-m_0},$$

$$m_0 = 0.5\{[0.5((16\gamma_0^4(c_1^{-1/2} - \operatorname{Re}_h^{-1/2})^{-4} + 1)^{1/2} + 1)]^{1/2} - 1\}. \tag{21}$$

Solutions in both the variants $K = K_0(1-x)^4$ and $K = K_0(1-x)^2$ are rather similar and are in good agreement with the numerical solutions cited in section 3. These solutions display an explicit dependence on outer parameters. The difference is in the functional dependence on depth: power and exponential. With the parameter β an explicit dependence of the basic characteristic on the ratio h/D is observed. This problem is singular and depth H is nothing but a characteristic of the coefficient K. Solutions have physical sense in the domain $[0, h]$. As the stratification parameter μ increases, the angle of rotation of the velocity vector tends to $\pi/2$ in the whole domain. Figure 6 illustrates the behavior of hydrodynamic characteristics as a function of the parameter μ for the following outer values $\operatorname{Re} = 10^4$, $\lambda = 10^4$ cm. As the value μ increases, the values h/D and γ, K_0 decrease, while the velocity module $|W_0|$ and the angle φ_0 at the surface $z = 0$ increase. It is seen that the solutions approach asymptotically of a neutrally-stratified variant when $\mu < 0.1$. The solutions proposed provide a realistic estimate of the UML characteristics known to us. Note that drift currents almost perpendicular to the wind direction in the UML have been recorded in situ (Lacomb et al. 1972).

In the solutions for shallow water (20), with depth H shoaling, drift velocities turn towards the wind direction in accordance with Ekman solution.

With an increase of the parameter μ, the coefficient

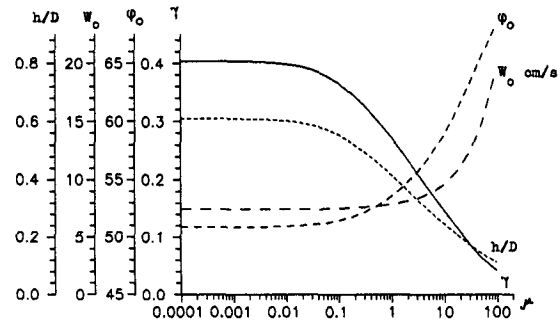

FIG. 6. Dependence of the values γ, φ_0, $|W_0|$, h/D on the stratification parameter μ for the solution $K = K_0(1-x)^2$.

K_0 and, hence, the depth of Ekman's friction layer D decrease, therefore beginning with a certain value of μ, these solutions (20) become unacceptable. An UML, of depth h smaller than the basin depth H, occurs for which the solutions above will become valid.

The suggested theory of drift friction layer in shallow water is fairly simple and physically conceivable, but it needs experimental verification. Here there is the preference of the linear velocity law to the conventional logarithmic law. The origin of the logarithmic law is traced back to the analytical solutions of Karman and Prandtl (Schlichting 1969) in hydrodynamics and up to now is still to be theoretically substantiated in geophysical hydrodynamics. The asymptotic formula of logarithmic velocity profile quoted in section 2 may be one of the examples.

5. Discussion

Empirical constants in $b - \epsilon$ model

$$c_{1\epsilon}\frac{\epsilon}{b}(P_S + c_{3\epsilon}P_b) + \left(\frac{K}{\delta_\epsilon}\epsilon_z\right)_z - c_{2\epsilon}\frac{\epsilon^2}{b} = 0, \quad (22)$$

$$K = c_\mu b^2/\epsilon, \quad (23)$$

$c_{1\epsilon}$, $c_{2\epsilon}$, $c_{3\epsilon}$, δ_ϵ, c_μ are not universal. (P_S is the shear term, P_b is the buoyancy force work). They are selected to investigate free turbulent flows outside regions of the laminar sublayer (Sukhorukov 1974; Kochergin and Sukhorukov 1975). Among them, most significant is the constant $c_{2\epsilon}$ whose variation limits are set by degenerate laws of homogeneous isotropic turbulence, $1.4 < c_{2\epsilon} < 2$. If $c_{2\epsilon}$ lie within this range, we have the finite depth of turbulence damping diffusing downward from the surface (K. L. Egorov, private communication). For turbulent motions in channels, the following constants were selected as optimal: $\delta_\epsilon = 1$, $c_{2\epsilon} = 1.9$, $c_\mu = 0.08$ (Kochergin and Sukhorukov 1975). To satisfy the conditions $h \approx 0.4u_*/f$ for the neutral stratified case, the value of $c_{2\epsilon}$ was taken equal to 1.4 in the problems of UML modeling (Kochergin et al. 1976).

The constants, termed c-constants, used by Rodi (1984), Omstedt et al.* (1983), and Kundu** (1980) are:

$c_{1\epsilon}$	$c_{2\epsilon}$	$c_{1\epsilon}c_{3\epsilon}$	c_μ	δ_ϵ	$^*c_{1\epsilon}c_{3\epsilon}$	$^{**}c_{1\epsilon}c_\epsilon$
1.45	1.92	1.45	0.09	1.3	0.8*	0.288**

Table 2 shows the results of numerical solutions of the stationary problem (1), (2), (11)–(14) with the c-constants used by Rodi, Omstedt et al. and Kundu, which model the deep ocean UML.

In these solutions, the velocity vector turns almost perpendicular to the wind as parameter μ increases. Values K, b, ϵ monotonically decrease with depth. However, the solutions turned out to be sensitive to the magnitude of the parameter μ even when its values are small, and in this range of values $\mu(\mu < 1)$, they differ essentially from those shown in Table 1. For example, depth h becomes greater than u_*/f. When $\mu > 1$ the distinction is less significant, though dissipation ϵ_0 differs essentially. The integral balance of the terms of the TKE equation is critically different as compared to that in Table 1. In it the contribution to potential energy dominates over dissipation which accounts for the solutions sensitivity to parameter μ even when its values are small. The ratio $\epsilon_I/(U_{10}u_*^2)$ does not exceed 0.1% which is less than experimental estimates—0.4% and 1.2% (Oakey 1985). The constant $c_{1\epsilon}c_{3\epsilon}$ becomes more important with an increase of parameter μ. Table 2 shows solutions at $\mu = 10$ where this constant takes the values 0.8 and 0.288. In this case, the solutions become more similar to those presented in Table 1; there occurs a change in the balance of terms ϵ_I and $g\alpha Qh$ and the ratio $\epsilon_I/(U_{10}u_*)$ increases.

The selection of constants in $b - \epsilon$ model should originate from the field data on the UML depth h and the TEC $K(z)$. The UML depth is conventionally believed to be determined by the relation $h \approx 0.4u_*/f$ ($\mu = 0$). Not arguing the validity of this relation, let us be careful about the value 0.4. Depth h is experimentally inferred from the temperature gradient creating the conditions of stable stratification, even if there is no heat flux at the surface. This temperature gradient may have a profound effect on the modeled depth h, particularly when the c-constants are used. Note that the formation of the jump of the density layer is an essentially nonstationary process (Marchuk et al. 1977).

Hence, of great interest are nonstationary prognostic calculations of natural meteo-information as compared with observations (Fridrich et al. 1981; Martin 1985; Sukhorukov et al. 1986). We have carried out numerical calculations with a nonstationary system of

TABLE 2. Calculated hydrodynamic values at different values of the parameter μ.

μ	1	10.	50.	100.	*10.	**10.
h/D	0.47	0.16	0.14	0.12	0.19	0.19
φ_0 (deg)	48.	79.	80.	80.	74.	73.
K_0 (cm^2 s^{-1})	1935	253	91	55	178	135
b_0 (cm^2 s^{-2})	1.7	1.7	1.5	1.3	2.3	2.4
ϵ_0 ($\times 10^{-3}$) (cm^2 s^{-3})	0.1	1.0	2.0	3.0	3.0	4.0
h (m)	92	11.5	6.0	4.0	11.5	10.0
$\epsilon_I/(u_0u_*^2)$ (%)	38	36	21	16	56	68
$g\alpha Qh/(u_0u_*^2)$ (%)	62	64	79	84	44	32
$\epsilon_I/(U_{10}u_*^2)$ (%)	0.07	0.07	0.08	0.09	0.18	0.27

Eqs. (1), (2), (11)–(14), to which the equation of heat transfer is added

$$T_t = \left\{ KT_z - \frac{F_i}{c_p \rho_0} [0.4 \exp(-a_1 z) + 0.6 \exp(-a_2 z)] \right\}_z, \quad (24)$$

boundary conditions of heat balance being estimated from hourly meteorological data at ocean station "C" for June 1979. In the turbulence equations the c-constants are used. We compared these calculations to the similar ones by Sukhorukov et al. (1986). In this work, a rather realistic prediction is obtained of the temperature field in the upper ocean layer. Compared solutions showed that the tendencies of stationary solutions given in Tables 1, 2 remain true. For example, if wind stress is greater than 1 dyn cm^{-2} the value of the coefficient K_0 is greater than 10^3 cm^2 s^{-1}, and depth h is likely to be two times larger than its observed values in extreme conditions. The accuracy of UML depth determination is restricted by temperature measured in the field at standard levels. Depth h being modeled reaches its maximum of 60 meters with wind stress equal to 2 dyn cm^{-2}. The mean value of the ratio $\epsilon_I/(U_{10}u_*^2)$ over the whole period of modeling is 0.1% as compared to 0.58% estimated by Sukhorukov et al. (1986). These calculations were made with a 15-min time step. Calculations using an hour time step and interative averaging of the K coefficient on this interval showed the discrepancy in the modeled depth h to become insignificant though discrepancy in the magnitude K_0 is still large: it is sometimes half an order greater than the values with the constant given by Sukhorukov (1974). In connection with this, note that even in the detailed calculations by Marchuk et al. (1977) the rate of deepening of the homogeneous layer depends on space and time steps and on the a priori value of the K-coefficient at the boundary $z = h$ and deeper. Thus, in a nonstationary problem with in situ data, the difference of constants in the model does not affect the modeled depth significantly.

Let us now address boundary conditions in the $b - \epsilon$ model ($Kb_z = 0$, $K\epsilon_z = 0$) implying the absence of turbulent fluxes from the wave-induced surface or symmetry conditions at $z = 0$.

For comparison, calculations similar to those presented in Table 2 were carried out with the c-constants and boundary conditions of the form:

B1) $z = 0$: $Kb_z = -u_*^3$, $\epsilon = P_S + P_b + (Kb_z)_z$;
B2) $z = 0$: $Kb_z = 0$, $\epsilon = P_S + P_b + (Kb_z)_z$;

which in the explicit form include a turbulent flux depending on wind stress (B1). The dissipation rate ϵ is a very changeable feature, hence, a priori boundary conditions for it or its flux and their inaccuracy may result in a severe error in the theoretical solution. The conditions of balance in B1, B2 are preferable in this sense, but the mathematical question about the solutions uniqueness remains to be answered. In both cases numerical experiments found that the velocity vector rotates nearly perpendicular to the wind direction as parameter μ increases. Magnitudes b and ϵ in solutions keep decreasing with depth and the $K(z)$ coefficient profile is governed by the conditions at $z = 0$. If the conditions $Kb_z = 0$, $K\epsilon_z = 0$ are satisfied, the $K(z)$ coefficient decreases monotonously with depth ($K_z = 2Kb_z/b - K\epsilon_z/\epsilon = 0$). If only the flux $Kb_z = 0$, then $K_z = -K\epsilon_z/\epsilon > 0 (\epsilon_z < 0)$ and $K(z)$ coefficient has its local maximum in the region. When the condition $Kb_z = -u_*^3$ is satisfied, the $K(z)$ coefficient may also reach its maximum in the region, which is verified by the calculations when $\mu < 10$; if $\mu > 10$, $K(z)$ coefficient takes on its maximum value at the boundary $z = 0$. The fact that the boundary $z = 0$ is deeper than the free surface does not conflict with the possibility for the $K(z)$ coefficient to take on its maxima values here. Pollard (1979) gives some estimates of values of the $K(z)$ coefficient which are on the order of 100 cm^2 s^{-1} and argues that its maxima values are near the sea surface. The UML depths h are almost the same in both the cases B1 and B2 ($\mu = 0.01$, $h = 150$ m) and at $\mu > 1$ are consistent with the values listed in Table 2. The magnitudes b_0, ϵ_0 exceed the values presented in Table 2, particularly in conditions B1. When $\mu > 1$, the solutions are more similar to those given in Table 1 and, in all the likelihood, more realistic

B1: $\mu = 1$: $K = 300$ cm^2 s^{-1}, $b_0 = 4$ cm^2 s^{-2}, $\epsilon_0 = 5 \times 10^{-3}$ cm^2 s^{-3}, $h = 55$ m, $\epsilon_I/(U_{10}u_*^2) = 0.7\%$.
B2: $\mu = 1$: $K = 200$ cm^2 s^{-1}, $b_0 = 3$ cm^2 s^{-2}, $\epsilon_0 = 4 \times 10^{-3}$ cm^2 s^{-3}, $h = 55$ m, $\epsilon_I/(U_{10}u_*^2) = 0.5\%$.

In our opinion, further investigations for determining the constants in the $b - \epsilon$ model are necessary to combine with the study of conditions at the ocean surface.

The idealized boundary condition at the base utilized in section 3 for shallow water $b_z = 0$, $\epsilon = P_S + P_b + (Kb_z)_z$, may be considered as a case of limiting roughness when the direct effect of the solid wall on turbulence is ruled out, its influence being realized by the condition $W = 0$. Or consider the case of a smooth bottom streamline beyond the region of a viscous sublayer when the velocity value should be given, taking into account the logarithmic law. Note that the bottom layer in a deep ocean is not similar to the one considered above.

We carried out numerical experiments, making allowance for the base roughness in a shallow water in the boundary conditions:

C1) $z = 0$: $Kb_z = 0$, $K\epsilon_z = 0$; $z = H$: $W = 0$, $b = \sqrt{K\epsilon/c_\mu}$, $\epsilon = P_S + P_b + (Kb_z)_z$, $K = \kappa z_0 u_*$;
C2) $z = 0$: $Kb_z = -u_*^3$, $\epsilon = P_S + P_b + (Kb_z)_z$; $z = H$: $W = 0$, $b = \sqrt{K\epsilon/c_\mu}$, $\epsilon = P_S + P_b + (Kb_z)_z$, $K = \kappa z_0 u_*$;

In the boundary conditions at $z = H$, only one assumption $K = \kappa z_0 u_*$ is introduced. Numerical experiments showed that in both cases with the c-constants, fairly realistic solutions are obtained as compared to those described in section 3. A decrease in depth H results in the phenomena stated by Theorem 2. The coefficient $K(z)$ increases from the bottom upward as is usually the case in turbulent flows near the wall. As the roughness length z_0 increases and depth H decreases, the $K(z)$ coefficient tends to become constant and the phenomena stated in Theorem 3 arise.

The phenomena stated in Theorems 1–3 are predicted by the $b - \epsilon$ model. Further investigations should be carried out such as a clarification of the role of boundary conditions for turbulence models aimed at the study of quantitative laws of the formation of boundary drift friction layers of the ocean.

6. Conclusion

Numerous solutions obtained over the 80 years of development of the stationary theory of drift currents made researchers conclude that the velocity hodograph is relatively insensitive to the shape of the VTE coefficient (Brown 1978). This is valid for large values of the ratio H/D and H/D_H, ($H/D > E$, E is the number introduced in section 2). For small values of H/D and H/D_H, whatever the $K(z)$ coefficient profile, the velocity hodograph is basically determined by the boundary condition at $z = H$: slip $KW_z = 0$ or no-slip condition $W = 0$. In this case, analytical solutions state that two fundamentally different types of motion can exist: velocities tend to turn orthogonal to (towards) the wind direction and friction stress components tend to be linear (constant) in the whole domain when a slip (no-slip) condition is satisfied at the boundary, respectively. These assertions were formulated as two theorems. One of them asserts a certain minimalization principle; the system tends to the minimum inflow of kinetic energy from the atmosphere to the ocean and, correspondingly, to turbulence. The other theorem validates the conditions under which constant friction stress exists. This fact is broadly used in hydrodynamics and geophysical hydrodynamics. The third theorem shows in a general form that the linear velocity profile is formed when the $K(z)$ coefficient tends to a constant value at small ratios H/D_H and a no-slip boundary condition. Under conditions of theorems 2, 3 theoretical grounds are given for the existence of the linear plus logarithmic velocity profile in the near bottom sublayer, which is well known in the surface layer of the atmosphere.

Numerical solution of turbulent drift friction layer of the ocean equations where the $K(z)$ coefficient was inferred from the equations of turbulent energy and turbulent dissipation, confirm the fact that these two types of motion can possibly exist. They demonstrate that the first type of motion manifests itself as the external dimensionless stratification parameter increases, which causes an increase in the oceans stable stratification. This type of motion is inherent in the UML. It is under such conditions, in summer, that drift currents almost orthogonal to the wind direction were observed in the upper layer of the Mediterranean (Lacomb et al. 1972). The second type of motion with the drift velocity towards the wind direction and with the layer of constant fluxes applies to shallow water where drift currents reach to the bottom. The conditions are discussed under which the formation of the linear velocity profile and constant values of turbulence characteristics are preferable in this case. These theoretical results need experimental testing.

Analytical solutions of the equations of the turbulent drift friction layer of the ocean for the two types of motion are constructed in elementary functions, where the effect of external parameters is clearly seen.

REFERENCES

Anderson, I., A. Huyer and R. L. Smith, 1983: Near-inertial motions off the Oregon Coast. *J. Geophys. Res.*, **88** (C10), 5960–5972.

Brown, R. A., 1978: Analytical methods of the simulations of planetary boundary layer. *Gidrometizdat,* USSR, Leningrad, 150.

Dmitriev, N. V., and V. A. Sukhorukov, 1982: Analytical Solution for the Ekman boundary ocean layer in function class of Bessel. *Chislennye Reshenij Zadach Dinamiki Oceana,* Novosibirsk, VC SO AN SSSR, 16 pp.

Dotsenko, S. F., 1971: On the question of drift current in the ocean at an arbitrary variation of the viscosity coefficient depending on depth. *Morskie Gidrofiz. Issledo.,* Sevastopol, 9 pp.

Fridrich, G., 1981: Numerical experiments on the model of the ocean. *Meteor. Gidrol.*, **7**, 77–85.

Ekman, V. W., 1905: On the influence of the Earth's rotation on Ocean. *Arkiv for Matimatik, Astronomi och Fisik,* **B2,** No. 11, 1–52.

Kazakov, A. L., and V. A. Sukhorukov, 1984: The estimate of effect meterological conditions parametrization in numerical modelling of the active layer of the ocean. *Chislennoe Reshenie Zadach Dinamiki Oceana i Vnutrennih Vodojomov,* VC SO AN SSSR, Novosibirsk, 21 pp.

Kitaigorodskii, S. A., M. A. Donelan, J. L. Lumley and E. A. Terray, 1983: Wave-turbulence interactions in the upper ocean part 2: Statistical characteristics of wave and turbulent components of the random velocity field in the marine surface layer. *J. Phys. Oceanogr.*, **13,** 1988–1999.

Kochergin, V. P., V. I. Klimok and V. A. Sukhorukov, 1976: Turbulent model of the Ekman layer of the ocean. *Chislennye Metody Mechaniki Sploshnoj Sredy,* Novosibirsk, Vol. 7, No. 1, 13 pp.

Kochergin, V. P., V. I. Klimok and V. A. Sukhorukov, 1977: Homogeneous layer of the ocean in terms of differential models. *Chislennye Metody Mechaniki Sploshnoj Sredy,* Novosibirsk, Vol. 8, No. 5, 13 pp.

Kochergin, V. P., and V. A. Sukhorukov, 1975: Two-parameter model of developed turbulence. *Chislennye Metody Mechaniki Sploshnoi Sredy,* Novosibirsk, Vol. 6, No. 5, 13 pp.

Kochergin, V. P., V. A. Sukhorukov and E. A. Tsvetova, 1974: Simulation of the processes of vertical turbulent diffusion in the ocean. *Chislennye Metody Rascheta Okeanskich Techenij.* Novosibirsk, 129–152.

Kondo, J., 1976: Parameterization of Turbulence in the Top Meter of the Ocean. *J. Phys. Oceanogr.* **6**(5), 712–720.

Kozlov, V. F., 1963: On the influence of the turbulent exchange coefficient on drift flows. *Jzv. AN SSSR, Ser. Geofiz.,* No. 7, 1100–1107.

Kullenberg, G., and R. Zaneveld, 1983: Aspect of Bottom Boundary

Layers in the ocean. *Struct and Dev. Greenland-Scotland Ridge: New Meth. and Conc. Proc. NATO Adv.*

Kundu, P. K., 1980a: A numerical investigation of mixed-layer dynamics. *J. Phys. Oceanogr.*, **10**, 220–236.

Kundu, P. K., 1980b: Reply. *J. Phys. Oceanogr.*, **10**, 1697.

Lacombe, H., B. Saint-Guily and J. Gonella, 1972: Observation of some effects in the sea brought about by density stratification on oceanic currents. *Wnytrennie Wolny w Oceane*, Novosibirsk, 7–23.

Marchuk, G. I., V. P. Kochergin, V. I. Klimok and V. A. Sukhorukov, 1977: On the dynamics of the ocean surface mixed layer. *J. Phys. Oceanogr.* **7**, 865–875.

——, V. P. Kochergin, V. I. Klimok and V. A. Sukhorukov, 1978: Mathematical modeling of seasonal change of the upper turbulent layer of the ocean. *Izv. Acad. Nauk USSR, Phizika Atmosphery Okeana*, **14**, 945–955.

——, V. P. Kochergin, V. I. Klimok and V. A. Sukhorukov, 1979: Analytical solutions for Ekman turbulent ocean layer. *Dokl. Akad. Nauk USSR*, **247**, 68–72.

Martin, P. J., 1985: Simulation of mixed layer at OWS November and Papa with several models., *J. Geophys. Res.*, **90**(C1), 903–916.

Mellor, G. L., and P. A. Durbin, 1975: The structure and dynamics of the ocean surface mixed layer, *J. Phys. Oceanogr.*, **5**(4), 718–728.

Mellor, G. L., and T. Yamada, 1974: A hierarchy of turbulence Closure Models for planetary boundary layers, *J. Atmos. Sci.*, **31**, 1791–1806.

Nikiforov, E. G., 1961: On the Theory of non-stationary currents in the conditions of multilayered sea. *Trudy AANII*, V. 210, USSR, Leningrad, 141–163.

Nomitsu, T., 1933: A theory of the rising stage of drift current in the ocean. *Memoirs of the College of Science Kyoto Imperial University*, **A16**(2–4), 161–175.

Oakey, N. S., 1985: Statistics of mixing parameters in the upper ocean during JASIN Phase 2. *J. Phys Oceanogr.*, **15**, 1662–1673.

Oakey, N. S., and J. A. Elliot, 1980: Dissipation in the mixed layer near Emerald Basin. Marine turbulence. *Proc. 11th Int. Colloq. Ocean Hydrod.* Liege, 123–133.

Omstedt, A., J. Sahlberg and U. Svensson, 1983: Measured and numerically-simulated autumn cooling in the Bay of Bothnia. *Tellus*, **35A**, 231–240.

Pollard, R. T., 1979: Observation and models of the ocean upper layer structure. *Modelirovanie i Prognoz Verhnih Sloev Okeana.* Leningrad, Gidrometeoizdat, 124–145.

Rodi, W., 1987: Examples of calculation methods for flow and mixing in stratified fluids. *J. Geophys. Res.*, **92**(C5), 5305–5328.

Rody, W., 1984: Environment turbulence model. In: Prediction methods for turbulent flows. Moskva, *Mir*, 227–322.

Schlixting, G., 1969: Theory of boundary layer. Moskow, *Nauka*, 742.

Sukhorukov, V. A., 1974: Weakly anisotropic transport processes in numerical calculations of viscous liquid dynamics. *Chislennye Metody Mechaniki Sploshnoj Sredy*, **5**, 108–119.

Sukhorukov, V. A., 1985: Vertical turbulent exchange modelling in the problems of the ocean dynamics. *MONOK, Trudy 1 Mezhdunarodnovo Simposiuma*, **3**, 288–294.

——, and N. V. Dmitriev, 1983: Accurate solution of equations of drift currents in the ocean. Preprint *VC SO AN SSSR 431*, Novosibirsk, 23.

——, and ——, 1984: To the theory of the drift friction layer of the ocean. *Chislennye Reshenija Zadach Dinamiki Okeana i Vnutrennih Vodojomov.* Novosibirsk, VC SO AN SSSR, 173–193.

——, and ——, 1986: Theory of stationary stable-stratified drift friction layer of the ocean. *Morskoj Gidrofizicheskij Jurnal*, **5**, 9–18.

——, and N. L. Tausnev, 1986: Numerical experiments with general circulation model of the North Atlantic. Preprint *VC SO AN SSSR 615*, Novosibirsk, 50.

——, ——, and S. M. Likhachev, 1986: Modeling upper mixed layer of the ocean. Preprint *VC SO AN SSSR 675*, Novosibirsk, 23.

Sundermann, J., V. I. Klimok, V. P. Kochergin, V. A. Sukhorukov and G. Fridrich, 1983: Numerical experiment on the general circulation model of the world ocean with an allowance for surface turbulence layer. In: *Materialy Sovetsko-francuzkogo Simpoziuma po Okeanografii 1*, Novosibirsk, 42–65.

Tricomi, F. 1962: Differential equations. *Moskow*, 351.